Heliyon 10 (2024) e30442

Contents lists available at ScienceDirect

Heliyon

journal homepage: www.cell.com/heliyon

Research article

Characterization of novel natural cellulose fiber from *Ficus macrocarpa bark* for lightweight structural composite application and its effect on chemical treatment

Jiratti Tengsuthiwat [a], Vinod A [b], Vijay R [b], Yashas Gowda T. G [c], Sanjay Mavinkere Rangappa [b,*], Suchart Siengchin [b]

[a] *Department of Mechanical Engineering Technology, College of Industrial Technology (CIT), King Mongkut's University of Technology North Bangkok (KMUTNB), Bangkok, Thailand*
[b] *Natural Composites Research Group Lab, Department of Materials and Production Engineering, The Sirindhorn International Thai-German Graduate School of Engineering (TGGS), King Mongkut's University of Technology North Bangkok (KMUTNB), Bangkok, Thailand*
[c] *Department of Mechanical Engineering, Malnad College of Engineering, Karnataka, India*

ARTICLE INFO

Keywords:
Cellulose
Characterization
Fiber
XRD
Ficus macrocarpa

ABSTRACT

This study investigates *Ficus Macrocarpa* tree bark fibers (FMB) as a sustainable alternative reinforcement for polymer composites. The Industrial Revolution marked the evolution of polymer composites with synthetic material reinforcement, leading to environmental concerns. Natural fibers have recently gained prominence as efficient alternatives for polymer composites. Despite numerous natural fibers being considered, ensuring a sustainable raw material source remains crucial. In this study, fibers were extracted from FMB and subjected to alkali treatment to evaluate their impact on physical, chemical, and thermal properties. Initially, the extracted fibers measured 253.80 ± 15 μm in diameter, reduced to 223.27 ± 12 μm post-alkali treatment. Chemical analysis showed an increase in cellulose content to 59.7 wt%, a 23.34 % improvement over untreated fibers (48.4 wt%). The crystalline index for untreated and treated fibers measured 80.20 % and 84.75 %, respectively, with no noticeable changes in the cellulose phase. Additionally, the crystalline size increased to 3.21 nm. Thermogravimetric analysis demonstrated enhanced stability of treated fibers up to 378.87 °C, while the kinetic activation energy remained constant at 64.76 kJ/mol for both the treated and the untreated fibers. The alkali treatment further improved surface roughness to 39.26, confirmed by scanning electron microscopic images. These findings highlight the potential of cellulose fibers from *Ficus Macrocarpa* bark as a sustainable and environmentally friendly replacement for synthetic fibers in polymer composites. The enhanced physical properties and excellent thermal stability make them a promising choice for eco-conscious materials.

1. Introduction

The growing need for environmentally friendly and sustainable materials has prompted the use of renewable resources for various engineering applications. Thus, natural fibers derived from plants have attracted considerable interest as a viable substitute for

* Corresponding author.
E-mail address: mavinkere.r.s@op.kmutnb.ac.th (S.M. Rangappa).

https://doi.org/10.1016/j.heliyon.2024.e30442
Received 18 December 2023; Received in revised form 25 April 2024; Accepted 26 April 2024
Available online 26 April 2024

synthetic fibers [1,2]. Moreover, these plant fibers possess several advantages, such as cost-effectiveness, ease of processing, eco-friendly, low density, and notable mechanical strength compared to synthetic counterparts [3]. These plant-based fibers are often called cellulose fibers and are derived from different parts of plants, such as leaves, stems, roots, and bark. These fibers comprise mainly hemicellulose, lignin, cellulose, pectin, wax, and other substances [1]. The chemical composition of these natural fibers is influenced by various factors, such as the plant's geographic location, the fiber extraction technique, and the exact section of the plant or tree from where it is extracted [4]. Notably, these chemical constituents play a significant role in determining the strength and thermal behavior of fibers [5].

Plant fibers have applications across various industries, including automotive manufacturing, aerospace, household products, civil engineering, and other sectors. These fibers have been extensively employed as strengthening components in polymer composites, contributing to producing soundproof panels, cargo pallets, doors, windows, and vehicle interior panels [6]. Recently, in various research in which the biomass obtained from the agricultural residues are used for die removal and the agricultural residues are hydrothermally treated to improve the fuel efficiency [7,8]. Moreover, the application of cellulose fibers obtained from plant sources has resulted in significant advancements within the packaging sector, leading to sustainability. The application suitability of the plant fibers is generally hindered by the moisture absorption nature and wettability issues of fibers with the matrix due to surface impurities [9,10].

Numerous surface treatment techniques, such as alkali, silane, oxalic acid, potassium permanganate, benzoyl chloride, corona, plasma, seawater, enzyme, etc., were employed to enhance the physical and chemical properties of plant fibers [11]. Literature indicates that chemical treatments are particularly effective in removing significant quantities of amorphous constituents like hemicellulose, pectin, lignin, wax, and impurities from the surface of the fibers by breaking down the hydroxyl groups. This removal substantially increases the cellulose-to-amorphous constituent ratio, thereby improving the performance properties of the plant fibers [12]. Additionally, chemical treatment makes the surface of plant fibers rougher. This enhanced roughness facilitates mechanical interlocking between the fiber and the matrix, thereby improving the fiber's wettability with the matrix. These improvements collectively enhance the performance of its usage in composites. Vinod et al. (2020) [13] investigated the performance characteristics of *Ziziphus mauritiana* fibers extracted from *Ziziphus mauritiana* (ZM) plant stems. The fibers were treated with 5 wt%/v of NaOH solution for 1 h. The alkali treated ZM fibers showed 1.2 times increment in the cellulose content with 1.31 times increment in the crystalline properties. The strength of the fibers after treatment also increased 1.44 times. This was effective performing upon its usage in the epoxy composite where the ultimate tensile strength increased 2.12 times for the alkali-treated ZM fiber-based composites Gurupranes et al. (2022) [14] studied the effect of alkali treatment on the *Ziziphus nummularia* fibers extracted from the *Ziziphus nummularia* barks. The fibers were treated for various soaking times ranging from 15 to 75 min in 5 wt%/vol. NaOH solution. The results showed that 5 wt% NaOH for 60 min duration treated fibers showed excellent results with 65.72 % cellulose contents, 50.6 % crystallinity index with good thermal stability up to 360 °C. Vijay et al. (2023) [15] characterized the *Vachellia farnesiana* fibers that were treated with alkali, hydrochloric acid and compared with raw fibers. The test results elucidated that alkali treatment effectively removed the amorphous constituents from the composition, thereby increasing the cellulose content ratio to 47.8 %. The thermal analysis using thermogravimetric analysis showed char residue of 39.5 % after 600 °C compared to untreated at 30.1 % and HCl treated at 28.9 %. The studies also revealed that HCl treatment removed more cellulose from the composition due to its acidic nature, causing poor results. It is inferred from the literature that optimal alkali concentration and soaking time using alkali can improve the physical

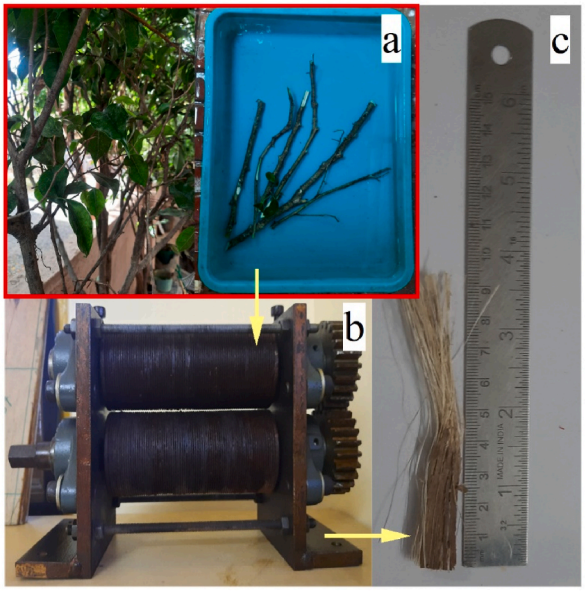

Fig. 1. Fiber extraction process (a) *Ficus Macrocarpa* plant stem (b) Mechanical retting (c) Extracted fibers.

and chemical qualities of plant fibers. As a result, the current study chose alkali treatment with optimal conditions as the preferred approach for treating *Ficus macrocarpa* bark fibers.

The worldwide market size of natural fiber-reinforced composites is projected to see a compound annual growth rate (CAGR) of 9.26 % from 2023 to 2028. This has led to a focus on discovering novel natural fibers for different applications. Despite the global exploration of various novel natural fibers by researchers, the demand, as given above, further increases the quest to find novel fibers. *Ficus macrocarpa* is a tropical tree with smooth, light-gray bark and oval-shaped leaves around 2–2.5 inches long. It may reach about forty feet (12 m) with a crown that spreads equally. The banyan tree thrives in tropical and humid subtropical environments where it may grow more significantly and have many prop roots. It is widely distributed in China, Tropical Asia and Australia. It is primarily an ornamental or shade plant. This research aims to explore the characteristics of fibers obtained from the bark of *Ficus macrocarpa* (FMB) and evaluate their suitability for reinforcement into lightweight structural composites. The extracted fibers were treated with 5 % NaOH solution to enhance its physico-chemical properties. The investigation involves an in-depth analysis of these fibers' physical, mechanical, and thermal properties to gain a comprehensive understanding of their potential as reinforcement materials. Furthermore, the study will investigate the impact of chemical treatment on fiber performance and its compatibility with the polymer matrix. This research aims to make a significant contribution to the field of sustainable materials by offering valuable insights into the practical use of *Ficus macrocarpa* bark fibers (FMB fibers) as an eco-friendly and viable option for structural composite materials.

2. Materials and methods

2.1. Fiber extraction and processing

The process of fiber extraction is presented in Fig. 1(a–c). Initially, Ficus Macrocarpa stems were collected following a pruning procedure. Subsequently, these pruned stems were cut to approximately 30 cm in length. The stems were immersed in water for a duration of 2 weeks to facilitate easy separation of the bark. After the soaking period, the barks were peeled from the stems, and the fiber extraction was done by passing the bark in between the two rollers. The obtained FMB fibers were then rinsed with distilled water to eliminate impurities and subsequently sun-dried to remove any remaining moisture content.

Previously, various research studies have revealed that a 5 % alkali treatment enhances the physico-chemical properties of natural fibers [9,16,17]. Therefore, in the current work, the fibers were treated with a 5 % alkali solution. NaOH solution with 5 % concentration was prepared by dissolving 53.77g of 98 % pure pellets of NaOH in deionized water until complete dissolution was achieved. The solution was diluted to make a final volume of 1000 ml. The alkali treatment process involved soaking 100g of FMB fibers in 1000 ml of 5 % NaOH solution while continuously stirring at room temperature (30 °C) for a duration of 4 h. Afterward, the treated fibers were rinsed in deionized water until the pH becomes normal. Subsequently, the fibers were dried in a hot air oven for 24 h at 60 °C to eliminate moisture.

During the alkali treatment, the hydroxyl groups on the fiber's surface were broken down, leading to removal of excess lignin, hemicellulose, pectin, wax and other impurities. Additionally, the NaOH solution penetrated the amorphous region, causing swelling of cellulose and enlarges the cell wall. This increased the surface roughness, creating a more accessible interface for plant fiber-resin interaction and promoting strong adhesion with the matrix through mechanical interlocking. Moreover, the alkali treatment caused the breakdown of fibers hydroxyl bonds that are sensitive, leading to the formation of hydroxyl bonds among molecules of cellulose. The enhanced moisture resistivity in plant fibers was due to the removal of hydroxyl groups that are sensitive to moisture. The untreated and treated fibers were designated as UT-FMB and T-FMB, respectively.

2.2. Physical analysis and chemical analysis

"Olympus BX43" was used to analyze the fiber's diameter of UT-FMB and T-FMB. The diameter was measured at 50 locations for both the untreated and treated FMB respectively. The statistical significance of the diameter values of UT-FMB and T-FMB were analyzed through Weibull statistical analysis. The density of the UT-FMB and T-FMB were determined through pycnometer experimentation. The chemical composition of the FMB fibers like cellulose, hemicellulose, and lignin were analyzed through chemical analysis. Kushner's and Hoffer's method as per NFT 12-008 was used to measure cellulose and hemicellulose composition. Klason's method as per APPITA P11s-78 was adapted to quantify the lignin content. The Conrad method was used to estimate the wax percentage. Fiber's moisture content was analyzed using an electronic moisture analyzer, "Sartorius MA45".

2.3. Fourier transforms infrared spectroscopy

Fourier Transform Infrared Spectroscopy (FTIR) was used to assess the impact of chemical treatment of chemicals on the functional groups in the FMB fibers. This experiment was conducted in the ATR (Attenuated Total Reflection) mode, employing 4 cm^{-1} resolution at 32 scans per minute, from 4000 cm^{-1} to 400 cm^{-1} using the FTIR machine "Invenio S, Bruker".

2.4. Thermogravimetric analysis

The thermal stability of the UT-FMB & T-FMB fibers were analyzed through thermogravimetric analysis (TGA). 7–8 mg of crushed FMB fibers were placed in a 70 µl of alumina crucible and the experiment was performed from 30 °C to 600 °C. The experiment was conducted using a heating rate of 10 °C/min and a nitrogen flow of 60 ml/min. Coat's Redfern equation was used to calculate kinetic

activation energy.

2.5. Differential scanning calorimetry

The differential scanning calorimetry (DSC) analysis [Machine: DSC 3+ STARe system, Mettler Toledo] was performed over the untreated and chemically treated FMB fibers to analyze enthalpy and heat flow within the fiber as a function of temperature change. 4–6 mg of crushed FMB fibers was placed in a 40 μl pan made up of aluminum. The experiment was performed from 30 °C to 450 °C with 50 ml/min nitrogen flow rate and 10 °C/min heating rate.

2.6. X-ray diffraction analysis

The impact of chemical treatment over the crystalline index and the crystal size of FMB fibers were evaluated using X-Ray diffraction (XRD) analysis. The experiment was performed using X-Ray diffraction machine "Smart Lab X-Ray diffractometer, Rigaku" and the experiment was performed in the 2θ range 10° to 50° with a step time of 5°/min. The crystalline index (C.I.) was calculated according to the equation $C.I. = [(I_{Cr} - I_{am})/I_{Cr}] \times 100$. The crystal size (CS) was calculated according to $CS = K\lambda/\beta \cos\theta$. Where I_{Cr} and I_{am} indicate the intensities of crystalline and amorphous contents. K denotes the Scherrer's constant (0.89), λ, and β is Bragg's angle, and the peak full width half maximum.

2.7. Mechanical analysis

The tensile strength of the UT-FMB and T-FMB fibers was analyzed through tensile test using INSTRON 5500R, USA according to ASTM 3822-07. The samples were tested with a 50 mm gauge length at a 2 mm/min speed. The test was conducted for 50 samples and the average values were reported.

2.8. Contact angle and surface roughness

The wettability behavior of UT-FMB and T-FMB fibers was analyzed using contact angle analysis. The experiment was performed on the FMB bark using "Contact angle analyzer, OCA 15Lj, Data physics" by dispensing 2 μl of liquid it and the capturing of images were done using camera with higher resolution after 10 s 20 readings were taken, and the average was reported. The values of contact angle were utilized to calculate the work of adhesion (WA) and the spreading coefficient (SC). The WA was calculated according to the Young-Dupré equation $W_A = \gamma_w(1 + \cos\theta)$, while the S_C was calculated according to the equation $S_C = \gamma_w(\cos\theta - 1)$. Where γ_w represents the water surface energy and contact angle is represented by θ. Image J software was used to plot the 3D surface roughness plot from the SEM images.

2.9. Morphological analysis and energy dispersive X-ray spectroscopy

The influence of chemical treatment over the fiber surface morphology was studied using the scanning electron microscopic images and elemental constitution was analyzed using EDX analysis. The SEM images were taken, and EDX was performed using the scanning electron microscope "ThermoFisher Scientific, Axia ChemiSEM". The samples were sputtered using gold, and the images were captured under a partial vacuum.

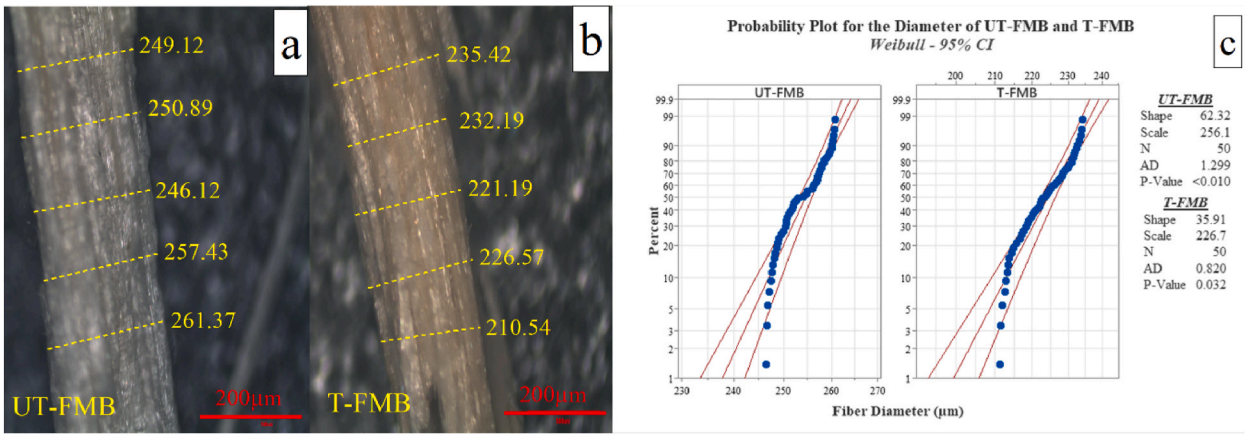

Fig. 2. Optical microscopic images (a) UT-FMB (b) T-FMB (c) Weibull distribution for the UT-FMB and T-FMB fiber.

3. Results and discussion

3.1. Physical and chemical analysis

Fig. 2 (a & b) depicts the optical microscopic images of UT-FMB and T-FMB. The average diameter values, chemical and physical properties of the treated and untreated fibers were presented in Table 1. Notably, the alkali treatment, using a 5 % NaOH solution, led to a significant reduction in fiber diameter, ranging from 210 to 240 μm, compared to the untreated fibers, which ranged from 245 to 265 μm. This reduction can be attributed to the alkali treatment's ability to break the hydroxyl bonds on the fiber surface, effectively removing impurities, waxy materials, and amorphous constituents which was present on the fiber surface [18]. Optical microscopic images Fig. 2 (a & b) of UT-FMB and T-FMB, presents diameter measurements with average values of 253.80 ± 15 μm and 223.27 ± 12 μm, respectively. The diameter of the UT-FMB was 1.12 times greater than those of T-FMB. The reduction of amorphous constituents resulted in the reduction of fiber diameter. This aligns with findings in the literature by Vinod et al., where the impact of various chemical treatments on *Muntingia Calabura fibers* was investigated [19]. The diameter values of the UT-FMB and T-FMB was subjected to Weibull analysis to study about the statistical significance of the values and presented in Fig. 2 (c). From the Weibull analysis, it was noted that the scale values of the UT-FMB and the T-FMB were approximately equal to the average diameter values respectively. Furthermore, it was noted that the P-values of both the fibers were less than 0.05, respectively. This indicated that there were significant differences in the diameter values of both the fibers, respectively. This phenomenon was because the diameter of the natural fibers will not be similar throughout the fiber. From the Weibull analysis, it was noted that the diameter of the UT-FMB falls within the range 246.42 μm–260.93 μm, while the diameter of T-FMB falls within the range 211.24 μm–234.31 μm. A similar behavior was observed in the studies conducted by Jawaid et al. [20] regarding oil palm-woven jute fiber-based composites. The density of the untreated and the treated fibers were measured and presented in Table 1. It was noticed that the density of T-FMB fibers increased by 1.05 times post-treatment compared to UT-FMB. The increase in density is attributed to the removal of a significant quantity of amorphous constituents from the fiber composition. As a result, this process brought the dense cellulose chains closer together, leading

Table 1
Comparison of physical and chemical properties of FMB fibers with other natural fibers.

Fiber Name	Diameter (μm)	Density (g/cc)	Cellulose (wt. %)	Hemicellulose (wt. %)	Lignin (wt. %)	Wax (wt. %)	Moisture (wt. %)	References
UT-FMB	253.80	1.245	48.4	12.2	14.3	2.5	10.1	Current work
T-FMB	223.27	1.312	59.7	8.1	6.8	0.9	5.3	Current work
Raw *Ziziphus nummularia* fiber	209.064	1322	52.34	18.64	13.43	0.63	10.45	[17]
Alkalized *Ziziphus nummularia* fiber	196.24	1352	65.72	8.22	7.78	0.41	7.80	
Untreated *Parthenium hysterophorus*	381.67	1251	51.5	9.7	14.3	2.8	8.6	[22]
Alkalized Parthenium *hysterophorus*	197.27	1360	56.1	4.5	10.8	0.7	5.3	
Untreated *Bambusa flexuosa*	140–175	0.81	56.68	16.19	18.93	1.22	5.7	[23]
Alkali treated *Bambusa flexuosa*	80–130	1.14	62.31	7.54	9.34	0.41	2.1	
Untreated *Capsicum annum* stem	0.92	1461.06	49.13	13.12	14.62	3.42	10.12	[24]
NaOH treated *Capsicum annum* stem	1.12	1214.96	54.27	7.25	8.32	0.79	7.12	
Untreated *Tridax procumbens*	233	1.16	32	6.8	3	0.71	11.2	[25]
NaOH treated *Tridax procumbens*	169.7	1.35	45	3.6	2.1	0.49	9.6	
Untreated Vachellia farnesiana	231	1270	38.3	12.1	9.2	3.4	11	[25]
NaOH treated Vachellia farnesiana	183	1352	47.8	7.3	4.7	1.8	6.3	
Untreated *Muntingia calabura*	148.29	0.921	41.5	11.3	7.6	3.4	6.1	[19]
NaOH treated *Muntingia calabura*	122.44	1.192	54.7	7.1	5.5	2.7	3.8	
Eleusine indica	315.4	1.143	61.3	14.7	11.12	2.9	5.6	[26]
Cardiospermum halicababum	310.12	1.140	59.82	16.75	9.3	1.3	1.9	[27]
Leucas aspera	335.1	1.118	50.7	13.2	9.7	–	11.31	[28]
Jute	40–350	1.46	61	13.6	12	0.5	12.6	[29]
Sisal	50–300	1.5	78	19	8	2	11	[30]

to an increased cellulose ratio relative to amorphous constituents. This structural change exerts a notable influence on the crystalline behavior of the fibers, a phenomenon similarly observed by Madhu et al. in their investigations on various chemical treatments of *Agave americana* fibers [21].

Cellulose is a complex carbohydrate polymer characterized by its long chains of glucose molecules linked together through beta-1,4 glycosidic bonds. It plays a fundamental role in conferring strength, stiffness, and stability to the fiber structure. While cellulose is resilient against hydrolysis, it can undergo degradation when exposed to certain chemical treatments. Hemicelluloses, on the other hand, are low-molecular-weight polysaccharides that often form disordered, amorphous, branched, or nonlinear structures. These polysaccharides are composed of glucose, glucuronic acid, mannose, arabinose, and xylose units. Lignin is an amorphous, cross-linked polymer network composed of a diverse array of hydroxy- and methoxy-substituted phenylpropane units, linked by various types of bonds. Its chemical composition varies depending on its source. The lignin is less polar than cellulose. It serves functions within and between fibers to enhance wall strength, regulate permeability, and facilitate water flow. Because of the stability of the aromatic rings in lignin, it is resistant to decomposition in anaerobic conditions and breaks down slowly in aerobic environments, making it generally resistant to microbial degradation [31]. From the chemical analysis, it was observed that T-FMB contained 59.7 wt% cellulose, whereas UT-FMB had 48.4 wt%. The increase in cellulose ratio was due to the removal of impurities and amorphous constituents by breaking down hydroxyl group, as seen in Table 1. These elevated cellulose ratios contributed to improved fiber performance, crystallinity, thermal stability, and mechanical performance, as further explained in the upcoming sections.

The reduction of amorphous constituents leads to a reduced hemicellulose ratio in the fibers, resulting in lower moisture retention in T-FMB compared to UT-FMB. Table 1 illustrates a more significant decrease in amorphous constituents in T-FMB due to the effective chemical treatment, as evidenced by reduced degradation phases in TGA and DSC results. A similar effect was observed in the study conducted by Vinod et al. on the influence of various chemical treatments on *Capsicum annum* stem fibers [24]. Furthermore, the chemical treatment results in reduced wax content, as evident from the contact angle results. This reduction in wax content promotes stronger bonding between FMB fibers and the matrix when used as reinforcement in composite development.

3.2. Fourier transform infrared spectroscopy

The Fourier transform infrared spectroscopy (FTIR) results for both UT-FMB and T-FMB were shown in Fig. 3, while the corresponding components of the fibers were presented in Table 2. The initial U transmittance peak, observed at the wavenumber range 3344 cm^{-1} and 3325 cm^{-1} for the untreated (UT-FMB) and chemically treated (T-FMB) FMB samples, respectively. This peak is attributed to the stretching vibration of O–H (hydroxyl groups), indicating the presence of cellulose [16]. The subsequent transmittance peak at wavenumbers 2914 cm^{-1} and 2921 cm^{-1} corresponds to the asymmetric stretching and vibration of CH_2 groups, indicating the presence of hemicellulose [32]. The following transmittance peaks observed at wavenumbers 1634 cm^{-1} and 1623 cm^{-1}, respectively for both the UT-FMB and T-FMB is an indicative for the stretching vibration of C═C bonds, which signifies the presence of lignin [24]. Another intensity peak observed at wavenumber 1510 cm^{-1} for UT-FMB indicates the stretching vibration of C═C bonds, associated with lignin and other aromatic components [2]. However, this peak was diminished in the spectrum of T-FMB due to the removal of considerable quantity of amorphous constituents. Similarly, a subsequent transmittance peak at wavenumber 1427 cm^{-1} in UT-FMB corresponds to the vibrations of methyl (CH_3) and methylene (CH_2) groups. This peak was decreased in T-FMB due to the removal of amorphous constituents. Transmittance peaks at wavenumbers 1230 cm^{-1} and 1227 cm^{-1} in both UT-FMB and T-FMB were attributed to vibrations in C–O bonds and bending vibrations of C–C–O, indicating the presence of hemicellulose and lignin. The final transmittance peaks at wavenumbers 1033 cm^{-1} and 1021 cm^{-1} for both untreated and treated FMB samples correspond to stretching and bending vibrations of C–O and C–*O*–C bonds, respectively [33]. These peaks were again attributed to the

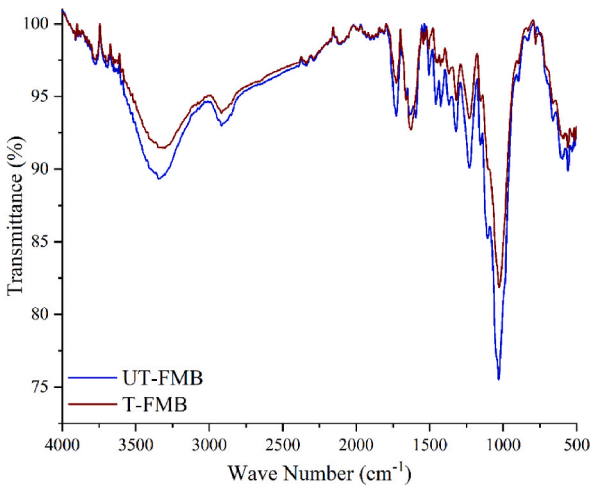

Fig. 3. Fourier transform infrared spectroscopy.

Table 2
Fourier transform infrared spectrograms and their corresponding wave number.

Fiber Designation		Wave number	Fiber component
UT-FMB	T-FMB		
3344	3325	stretching vibration of O–H (hydroxyl) groups.	Cellulose
2914	2921	asymmetric stretching vibration of CH2 groups	Hemicellulose
1634	1623	C═C stretching vibration,	Lignin
1510	1513	C═C stretching vibration	Lignin, and other aromatic compounds
1427	–	Vibration of methyl (CH_3) and methylene (CH_2) groups	Cellulose, hemicellulose, and lignin,
1230	1227	Vibrations of the C–O bond and C–C–O bending vibrations	Hemicellulose, and lignin
1033	1021	C–O stretching vibrations and C–*O*–C bending vibrations	Hemicellulose, and lignin

presence of amorphous constituents such as hemicellulose and lignin present in the fiber.

3.3. X-ray diffraction analysis

The X-ray Diffraction (XRD) analysis of both UT-FMB and T-FMB fibers was depicted in Fig. 4 (a, b), while the corresponding XRD data were presented in Table 3. The XRD graphs showed two distinct intensity peaks within the 2θ range, specifically at 15° and 22°. These peaks are typical for cellulose plant fibers and signify the presence of crystalline cellulose. The untreated and treated FMB fibers exhibited intensity peaks at approximately 15.43° and 15.44°, respectively. These peaks correspond to the lattice planes 1 1 0 and indicate the existence of cellulose 1β [34,35]. Additionally, prominent intensity peaks at around 22.39° and 22.84°, corresponding to the lattice plane 2 0 0, further confirming the presence of crystalline cellulose 1β [36,37]. Evidently, the chemical treatment did not induce any transformative changes in the cellulose, as the lattice planes remained consistent in the treated FMB fibers when compared to the untreated FMB fibers. The region between the valleys of the two crystalline cellulose peaks, around 2θ 18.83°, was identified as the amorphous region [24]. To calculate the crystalline index, Segal's method was employed for both untreated and chemically treated samples. According to the Segal's equation the crystalline index of the untreated and the chemically treated FMB fibers were estimated to be 80.20 % and 84.75 %, respectively. Notably, the crystalline index increased up to 5.67 % due to the chemical treatment. This increase in the crystalline index can be attributed to the removal of amorphous constituents from the fibers during the chemical treatment. Consequently, the weight ratio of crystalline cellulose increased relative to the amorphous constituents in the fibers. The crystalline index was again calculated using the de-convolution method and presented in Table 3. For the untreated FMB fibers the crystal size (CS) associated with the dominant cellulose peaks revealed sizes of 2.49 nm and 2.93 nm for the 2θ regions of 15.43° and 22.39°, respectively. Similarly, the crystal sizes of treated FMB fibers at 15.44° and 22.84° were measured as 2.56 nm and 3.21 nm. Remarkably, the chemical treatment led to a notable increment in the crystal size of FMB fibers. This phenomenon has an interesting implication: an enlarged crystal size corresponds to reduced water absorption capacity when these fibers are employed as reinforcement in composites. Moreover, the increase in the crystalline index increases the stiffness and mechanical strength of the fibers.

3.4. Thermogravimetric analysis

The thermogravimetric analysis of both UT-FMB and T-FMB was presented in Fig. 5 (a – d), while the corresponding analytical data

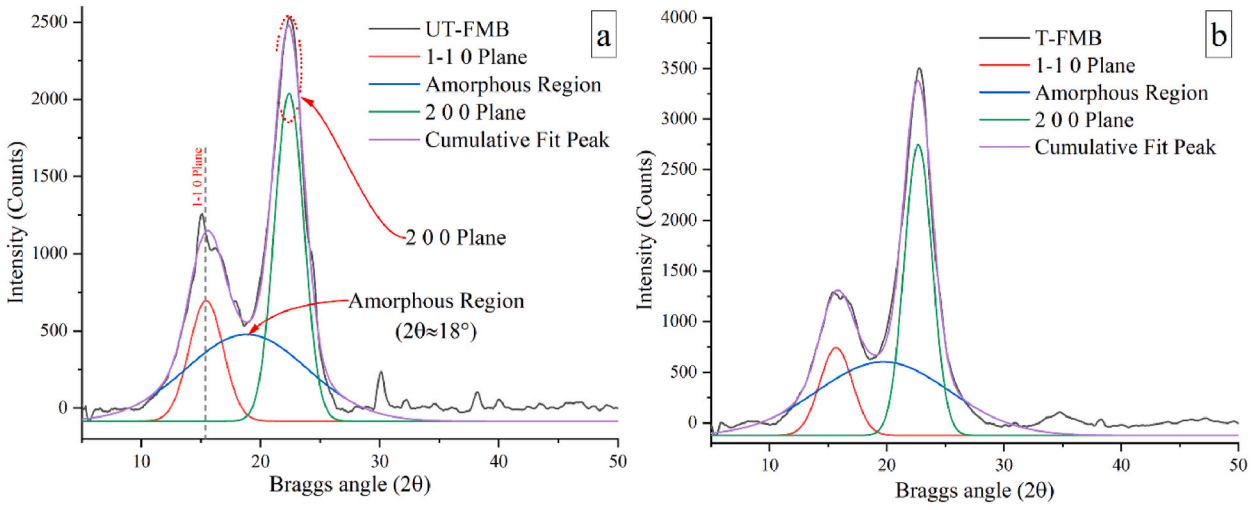

Fig. 4. X-Ray diffraction analysis (a) Untreated FMB fiber (b) Treated FMB fiber.

Table 3
X-Ray diffraction analysis data.

Fiber	Diffraction angle (2θ)	Intensity (Counts)	FWHM	Lattice h k l	CI Segal (%)	CI De-Conv (%)	CS (nm)	Allomorph
UT-FMB	15.43°	1208	3.36	I–I 0	–	–	2.49	Cellulose - 1β
	22.39°	2522	2.89	2 0 0	80.20	78.09	2.93	Cellulose - 1β
	18.83°	542	–	–	–	–	–	Amorphous
T-FMB	15.44°	1290	3.27	I–I 0	–	–	2.56	Cellulose - 1β
	22.84°	3610	2.64	2 0 0	84.75	80.78	3.21	Cellulose - 1β
	18.72°	549	–	–	–	–	–	Amorphous

is summarized in Table 4. Initial weight loss in the untreated FMB fiber occurred at 110.16 °C, resulting in an 8.71 % weight loss. In contrast, the treated FMB fibers exhibited a weight loss of 6.98 % at a slightly higher temperature of 121.36 °C. This initial phase of degradation was attributed to the evaporation of structurally integrated water molecules within the fiber [38]. The lower weight loss % and the higher $T_{initial}$ value represents the lower moisture content in the fibers due to the removal of considerable amount of hemicellulose during the chemical treatment. The next phase of thermal degradation, known as T_{Onset}, occurred at the temperature span of 230.52 °C for the UT-FMB fibers and 238.01 °C for the treated fibers. This degradation stage resulted in an weight losses of 5.35 % and 2.67 % respectively, signifying the breakdown of hemicellulose, wax, and other amorphous constituents present in the fiber [39]. Notably, this stage demonstrated a lower weight loss for the chemically treated FMB fibers compared to the untreated FMB fibers. This variance was due to the lower ratio of amorphous material resulting from the chemical treatment that significantly reduced the amorphous wt.% on the fiber surface. The final degradation stage, referred to as T_{Final}, occurred at the temperature of 351.12 °C for untreated fibers and 372.83 °C for the chemically treated fibers [40]. This stage marked the degradation of cellulose within the fiber. At this point, the weight loss percentage was higher for the treated FMB fibers due to the higher wt.% of cellulose present in them,

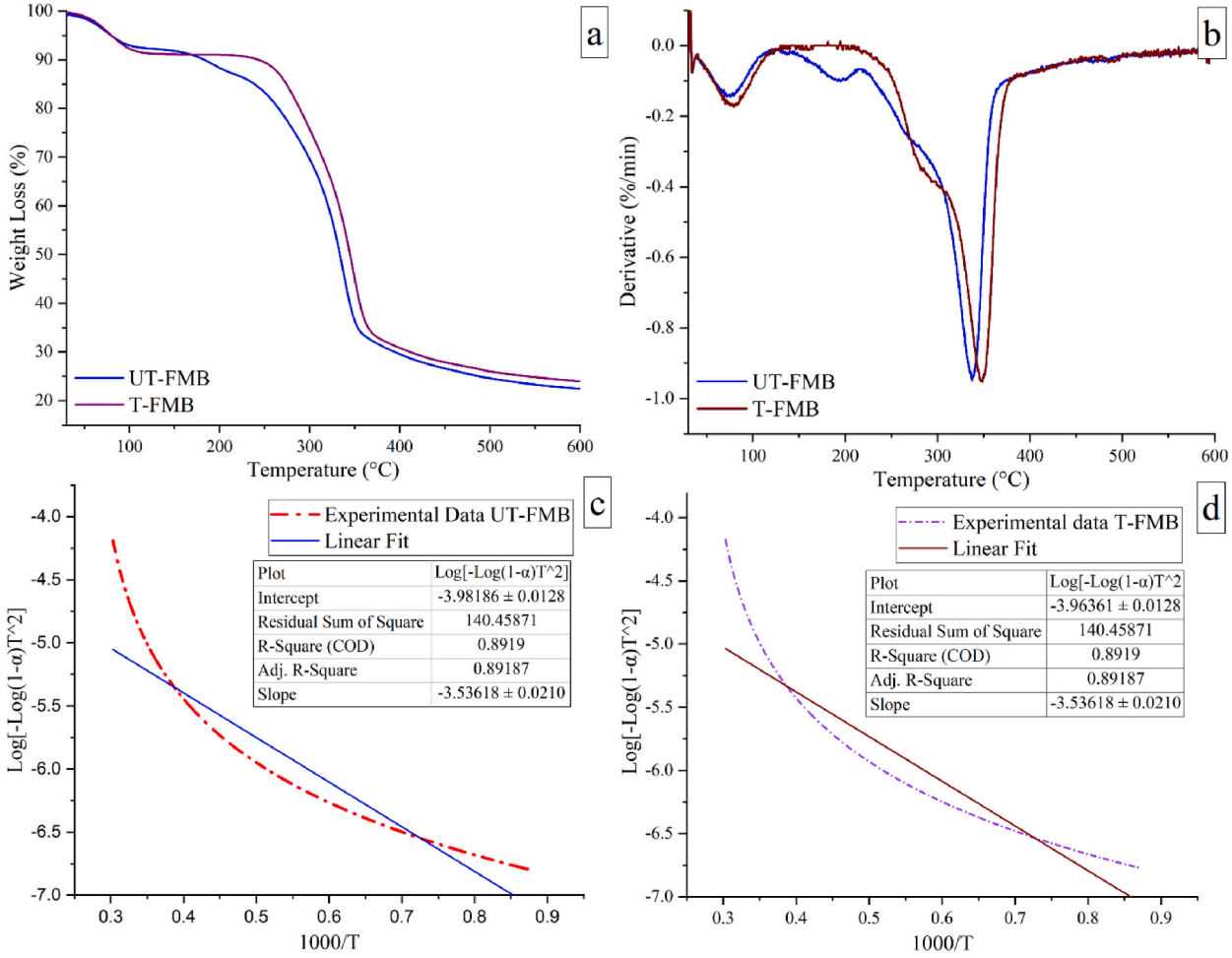

Fig. 5. Thermogravimetric analysis of the FMB fiber. (a) TGA curves (b) DTG curves (c and d) Kinetic plot Log[-Log(1-α) T^2] vs 1000/T for Ea.

Table 4
Thermal properties of the untreated and chemically treated FMB.

Fiber	$T_{Initial}$ (°C)	Wt. loss (%)	T_{Onset} (°C)	Wt. loss (%)	T_{Final} (°C)	Wt. loss (%)	Thermal Stability (°C)	Maximum degradation temperature (°C)	Kinetic activation energy (kJ/mol)
UT-FMB	110.16	8.71	230.52	5.25	351.12	29.63	240.01	362.43	64.76
T-FMB	121.36	6.98	238.01	2.67	372.83	34.69	249.37	373.87	64.76

Char residue UT-FMB 22.48; T-FMB 24.16.

because of the chemical treatment. The thermal stability of the T-FMB fibers was determined to be 249.37 °C, while the untreated fibers exhibited a thermal stability of 240.01 °C. The maximum degradation temperatures for the untreated and treated FMB fibers were 362.43 °C and 373.87 °C respectively. The kinetic activation energy for both untreated and chemically treated fibers was found to be 64.76 kJ/mol. This kinetic activation energy parameter represents the energy required for the sample to initiate thermal decomposition [24]. It was noted that the kinetic activation energy remained consistent due to the uniform slope of thermal degradation for both cases.

3.5. Differential scanning calorimetry

The differential scanning calorimetry analysis was presented in Fig. 6, and the analysis data were shown in Table 5. From the DSC curves, the first endothermic peak was observed in the range of 92.39 °C for both untreated and treated FMB, indicating the presence of structurally integrated moisture in both the samples. This peak was an endothermic peak, and the UT-FMB exhibited the highest ΔH value of 210.37 J/g, which was higher compared to the T-FMB fibers. This difference was attributed to the higher moisture content in the UT-FMB due to a higher hemicellulose ratio [41]. The next endothermic peak was observed in the range of 242.96 °C for the UT-FMB and 254.65 °C for the T-FMB, representing the degradation of amorphous constituents present in the fiber. Similarly, it was noted that the ΔH values of the untreated fiber was 64.3 J/g and was higher when compared to the T-FMB due to the presence of more amorphous constituents [42]. It was evident that the chemical treatment significantly reduced the amorphous constituents by breaking the hydroxyl groups. The subsequent endothermic peak occurred in the temperature range of 329.32 °C for the untreated fiber and 331.64 °C for the T-FMB fibers, with enthalpy values of 26.93 J/g and 31.36 J/g for the UT-FMB and T-FMB, respectively. The higher ΔH values in the T-FMB fibers were attributed to the higher ratio of cellulose compared to amorphous constituents [43]. Consequently, more energy was required for the degradation of cellulose. The final stage of degradation was observed beyond 375.88 °C for both UT-FMB and T-FMB, respectively.

3.6. Mechanical analysis

The tensile analysis of the UT-FMB and T-FMB were presented in Fig. 7. From the stress-strain curves the tensile strength of UT-FMB was 36.1±5 MPa, upon chemical treatment the tensile strength increased up to 47.3±3 MPa. The alkali treatment improved the tensile strength up to 1.31 times. This improvement in tensile performance resulted from the removal of a significant amount of amorphous constituents through chemical treatment, leading to a denser arrangement of cellulose chains. Such a structural change directly influenced stiffness and tensile performance, a behavior previously observed in studies involving chemically treated *Capsicum annum* and *Tridax Procumbens* [24,25]. The enhanced tensile strength values play a crucial role in facilitating effective stress transfer when these fibers serve as reinforcement in a polymer matrix. Notably, the strain for T-FMB measured 0.017, while UT-FMB exhibited a strain of 0.022. The reduced strain in T-FMB can be attributed to the NaOH treatment, which diminished the amorphous constituents, imparting greater stiffness to the fibers. This reduction in strain is advantageous for decreasing strain in composite materials under load, thereby enhancing their strength performance. The tensile modulus of the UT-FMB and T-FMB were 1.6 GPa and 2.73 GPa, respectively. During tensile loading, T-FMB fibers exhibited brittle fracture characteristics which was due to the increased stiffness due to the alkali treatmetn. Initially, there was quasi-linear deformation during strain, followed by non-linear deformation. The initial slope represented quasi-linear elastic loading, while the subsequent non-linear deformation during fracture was primarily caused by fiber cell delamination and the collapse of the weaker primary cell wall. Similar behavior was reported in the investigation of the tensile behavior of Calamus manan fibers for potential reinforcement in polymer matrix composites [38]. The obtained tensile strength

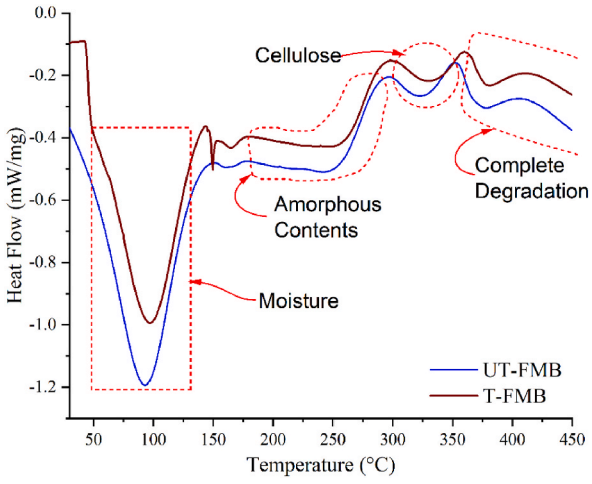

Fig. 6. Differential scanning calorimetry analysis.

Table 5
Differential scanning calorimetry peak data.

Fiber	Temperature (°C)	Peak type	ΔH (J/g)
UT-FMB	93.39	Endothermic	210.37
	242.96		64.3
	322.92		26.93
	375.88		Complete degradation
T- FMB	97.03		186.78
	254.65		41.27
	331.64		31.36
	379.52		Complete degradation

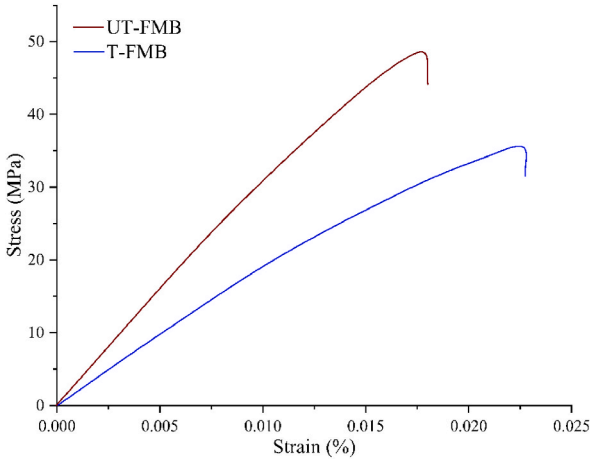

Fig. 7. Tensile stress-strain curve.

values were found to be higher than those of *Passiflora foetida* (0.44 MPa) and NaOH *Muntingia calabura* (26.74 MPa), yet lower than *Calamus manan* fibers (273.28 MPa) and *Capsicum annum* stem fibers (48.76 MPa) [44].

3.7. Contact angle and surface roughness

The contact angle analysis of the UT-FMB and T-FMB was depicted in Fig. 8 (a & b), while surface roughness analysis was presented in Fig. 8 (c & d). The corresponding data were summarized in Table 6. The untreated FMB fibers exhibited a contact angle of 83.5°, whereas the treated FMB fibers had a reduced contact angle of 76.9°. This reduction in contact angle, by 7.9 %, is due to the alkali treatment, which caused the disintegration of some fiber components and amorphous constituents on the fiber surface [9]. This decrease in contact angle can be attributed to the removal of nonpolar materials such as wax and impurities during the alkali treatment, enabling liquids to spread more efficiently across the fiber surface compared to untreated FMB fibers [2]. This improved wetting behavior is advantageous when these fibers are used as reinforcements in a polymer matrix. The work of adhesion represents how well the liquid can stick towards the solid surface, while the spreading coefficient represents how well the liquid can spread over the fiber surface. In the current work the analysis is performed using distilled water. From Table 6, the W_A value of the UT-FMB and T-FMB fibers were 80.15 and 88.31, respectively. The higher W_A for the T-FMB represents the good adhesion of liquid over the fiber surface, due to the removal of nonpolar substances from the fiber surface through chemical treatment. This phenomenon further improves the spreading coefficient, where the T-FMB exhibited higher spreading coefficient when compared to the UT-FMB.

Furthermore, 3D roughness profiles were generated using image J to analyze the changes in fiber surface morphology resulting from the chemical treatment. These profiles were constructed from SEM images and were presented in Fig. 8 (c & d). The average roughness (Ra) and root mean square (Rq) values were calculated using ImageJ software and were presented in Table 6. The untreated fibers exhibited a lower surface roughness of 41.52, while the alkali treatment increased the surface roughness to 46.98. This increase in roughness is a consequence of the chemical treatment, which led to the disintegration of the fiber surface [24].

3.8. Morphological analysis

The SEM images of UT-FMB and T-FMB can be found in Fig. 9 (a & b). In Fig. 9 (a), the SEM image reveals the presence of impurities, non-polar materials and wax, which are the primary reasons behind the lower wettability of the fibers. This was evident from the contact angle results, which showed higher contact angle values. Additionally, the images show that the fibers exhibit microcracks and voids, factors that could hinder the composite's performance when used as reinforcement in polymeric composites. This behavior

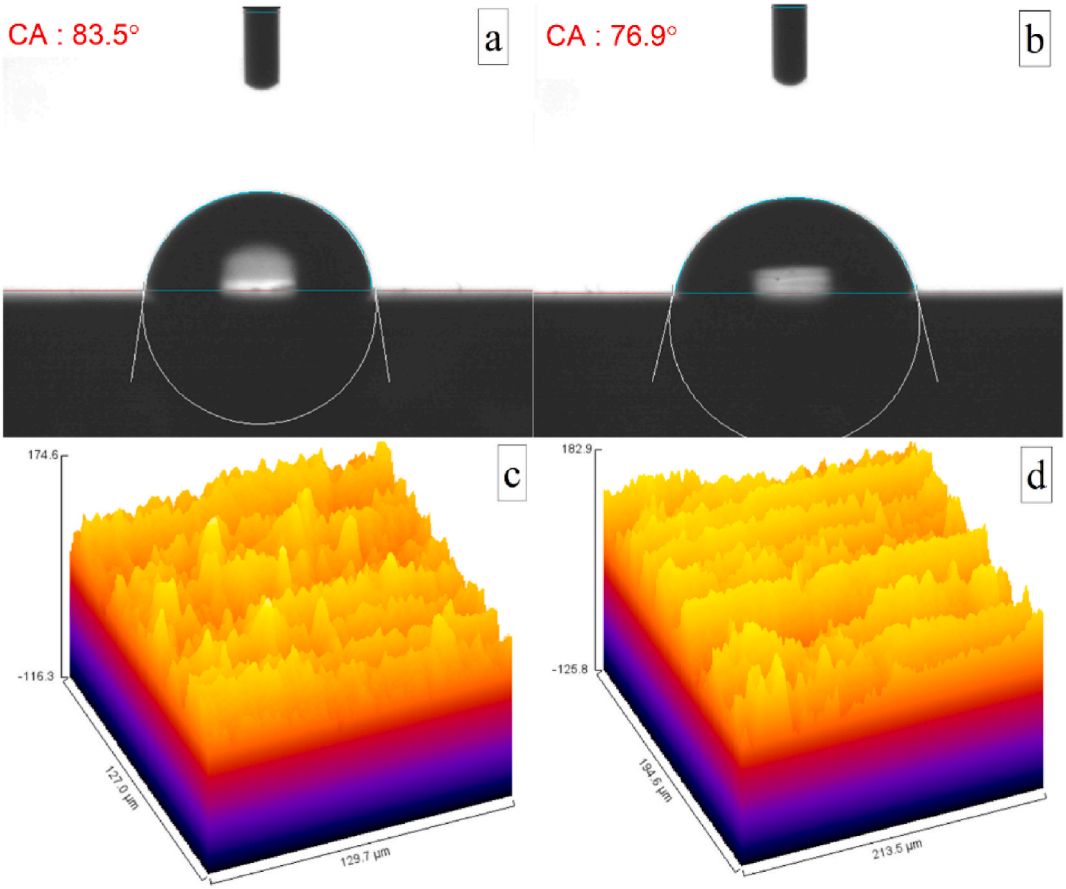

Fig. 8. (a) UT-FMB (b) T-FMB; 3D-surface plots (c) UT-FMB (d) T-FMB.

Table 6
Contact angle analysis of UT-FMB and T-FMB.

Fiber designation	Contact Angle (θ)	Root Mean Square Roughness (R_q)	Average Roughness (R_a)	Work of Adhesion (W_A)	Spreading Coefficient (S_C)
UT-FMB	83.5°	41.52	33.52	80.15	−63.84
T-FMB	76.9°	46.98	39.26	88.31	−55.68

aligns with the morphological findings of *Coccinia grandis* stem fibers [45]. The SEM image of T-FMB fibers in Fig. 9 (b) demonstrate a significant reduction in impurities and non-polar materials, resulting in reduced contact angle values (Fig. 8 (b)) and increased surface roughness. This transformation is evident from the contact angle and surface roughness analyses. The treated T-FMB fibers now exhibits a rougher surface which features to facilitate better interlocking with the matrix when used in polymeric composites, owing to the breaking of hydroxyl groups from fiber surface through chemical treatment. Furthermore, the chemical treatment has successfully eliminated cracks and impurities, which contributes to maintaining mechanical strength [25].

4. Conclusion

The experimental analysis concludes that the fibers extracted from Ficus Macrocarpa bark fibers can be used as potential alternative reinforcements in the polymer composites. The utilization of a 5 % alkali solution for chemical treatment proves to be particularly effective in enhancing the physical, chemical, thermal, and mechanical properties of FMB fibers. The treatment process results in surface disintegration, rendering the fibers rougher and reducing their diameter to 223.27 µm. The chemical treatment disintegrated the fiber surface, making it rough and reduced the fiber diameter up to 223.27 µm. Chemical analysis confirmed an increased cellulose weight % of 59.7 wt% and significant reductions in amorphous constituents like hemicellulose, lignin, and wax to 8.1 wt%, 6.8 wt%, and 0.9 wt%, respectively. This improvement in the chemical property enhanced the FMB's crystalline index (84.75 %) and increased the crystalline size up to 3.21 nm. A higher crystalline size reduces the water permeability within the fibers when used as

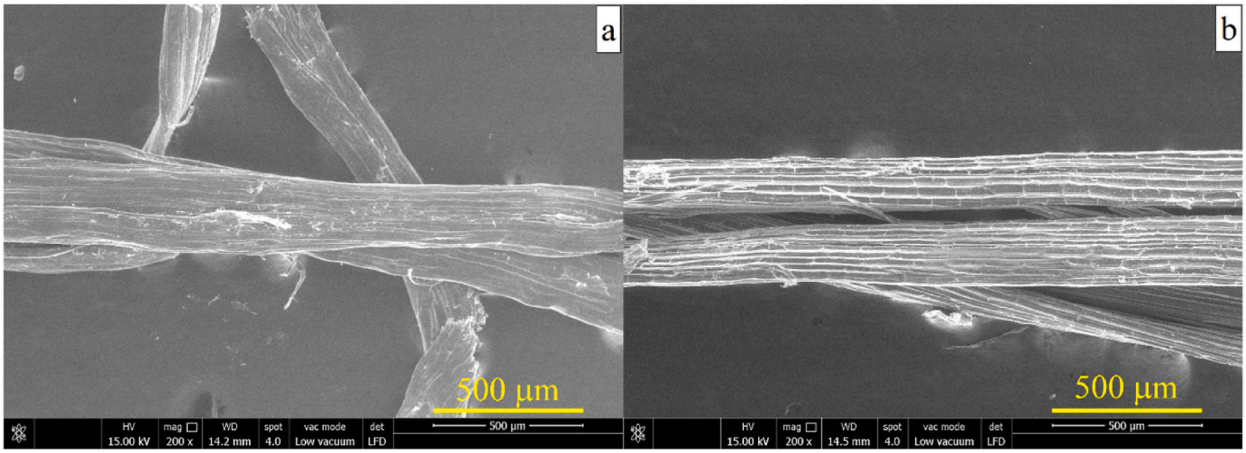

Fig. 9. Scanning electron microscopic images (a) UT-FMB (b) T-FMB.

reinforcements in polymer composites. Mechanical results further support these findings, indicating that the higher cellulose content enhances the fiber's tensile strength up to 47.3 MPa. Thermal analysis reveals increased thermal stability attributed to the removal of low thermally stable amorphous constituents, while the activation energy remains consistent at 64.76 kJ/mol for both untreated and treated FMB fibers. Morphological and contact angle analyses conclude that the heightened fiber surface roughness improves wettability, as evidenced by the Wa and Sc values, respectively. This enhancement facilitates superior interfacial adhesion between the fibers and matrix. From the results it was concluded that the Ficus Macrocarpa fibers represent a promising alternative source of raw material that can be potentially used as reinforcements in polymer composites.

CRediT authorship contribution statement

Jiratti Tengsuthiwat: Writing – review & editing, Writing – original draft, Visualization, Validation, Methodology, Investigation, Formal analysis, Data curation, Conceptualization. **Vinod A:** Writing – review & editing, Writing – original draft, Visualization, Validation, Methodology, Investigation, Formal analysis, Data curation, Conceptualization. **Vijay R:** Writing – review & editing, Writing – original draft, Visualization, Validation, Methodology, Investigation, Formal analysis, Data curation, Conceptualization. **Yashas Gowda T. G:** Writing – review & editing, Visualization, Formal analysis, Data curation, Conceptualization. **Sanjay Mavinkere Rangappa:** Writing – review & editing, Writing – original draft, Visualization, Validation, Supervision, Software, Resources, Project administration, Methodology, Investigation, Funding acquisition, Formal analysis, Data curation, Conceptualization. **Suchart Siengchin:** Writing – review & editing, Visualization, Validation, Supervision, Software, Resources, Project administration, Methodology, Funding acquisition, Formal analysis, Conceptualization.

Declaration of competing interest

The authors declare the following financial interests/personal relationships which may be considered as potential competing interests:The Corresponding Author of this paper, Sanjay Mavinkere Rangappa, works as an Associate Editor at Heliyon Materials Science.

Acknowledgement

This research was funded by King Mongkut's University of Technology North Bangkok with Contract no. KMUTNB-67-KNOW-27.

References

[1] E. Syafri, A. Vinod, R. Vijay, M.R. Sanjay, S. Siengchin, Green materials - the advancements and applications of natural fibers, J. Fibers Polym. Compos. 2 (2023) 168–173, https://doi.org/10.55043/jfpc.v2i2.130.
[2] A. Vinod, M.R. Sanjay, S. Suchart, P. Jyotishkumar, Renewable and sustainable biobased materials: an assessment on biofibers, biofilms, biopolymers and biocomposites, J. Clean. Prod. 258 (2020) 120978, https://doi.org/10.1016/j.jclepro.2020.120978.
[3] V.E. Ogbonna, A.P.I. Popoola, O.M. Popoola, A Review on Recent Advances on the Mechanical and Conductivity Properties of Epoxy Nanocomposites for Industrial Applications, Springer Berlin Heidelberg, 2023, https://doi.org/10.1007/s00289-022-04249-4.
[4] O. Akatwijuka, M.A.H. Gepreel, A. Abdel-Mawgood, M. Yamamoto, Y. Saito, A.H. Hassanin, Overview of banana cellulosic fibers: agro-biomass potential, fiber extraction, properties, and sustainable applications, Biomass Convers. Biorefinery (2022), https://doi.org/10.1007/s13399-022-02819-0.
[5] Y. Seki, F. Selli, Ü.H. Erdoğan, M. Atagür, M.Ö. Seydibeyoğlu, A Review on Alternative Raw Materials for Sustainable Production: Novel Plant Fibers, Springer Netherlands, 2022, https://doi.org/10.1007/s10570-022-04597-4.
[6] M. Akter, M.H. Uddin, H.R. Anik, Plant Fiber-Reinforced Polymer Composites: a Review on Modification, Fabrication, Properties, and Applications, Springer Berlin Heidelberg, 2023, https://doi.org/10.1007/s00289-023-04733-5.

[7] Y. Yu, A. Lau, S. Sokhansanj, Improvement of the pellet quality and fuel characteristics of agricultural residues through mild hydrothermal treatment, Ind. Crops Prod. 169 (2021) 113654, https://doi.org/10.1016/j.indcrop.2021.113654.

[8] Y. Xia, H. Zuo, J. Lv, S. Wei, Y. Yao, Z. Liu, Q. Lin, Y. Yu, W. Yu, Y. Huang, Preparation of multi-layered microcapsule-shaped activated biomass carbon with ultrahigh surface area from bamboo parenchyma cells for energy storage and cationic dyes removal, J. Clean. Prod. 396 (2023) 136517, https://doi.org/10.1016/j.jclepro.2023.136517.

[9] M. Mohammed, R. Rahman, A.M. Mohammed, B.O. Betar, A.F. Osman, T. Adam, O.S. Dahham, S.C.B. Gopinath, Improving hydrophobicity and compatibility between kenaf fiber and polymer composite by surface treatment with inorganic nanoparticles, Arab. J. Chem. 15 (2022) 104233, https://doi.org/10.1016/j.arabjc.2022.104233.

[10] R. Koundal, R. Khanduja, A. Sharma, K. Singh, A review of natural fiber-reinforced polymer composite chemical, physical, and thermo-mechanical properties, J, Fibers Polym. Compos. 1 (2023) 67–80, https://doi.org/10.55043/jfpc.v2i2.130.

[11] A. Hasan, M.S. Rabbi, M. Maruf Billah, Making the lignocellulosic fibers chemically compatible for composite: a comprehensive review, Clean. Mater. 4 (2022) 100078, https://doi.org/10.1016/j.clema.2022.100078.

[12] K.R.J. Sheeba, R.K. Priya, K.P. Arunachalam, S. Avudaiappan, N. Maureira-Carsalade, Á. Roco-Videla, Characterisation of sodium acetate treatment on Acacia pennata natural fibres, Polymers 15 (2023), https://doi.org/10.3390/polym15091996.

[13] A. Vinod, R. Vijay, D. Lenin Singaravelu, A. Khan, M.R. Sanjay, S. Siengchin, F. Verpoort, K.A. Alamry, A.M. Asiri, Effect of alkali treatment on performance characterization of Ziziphus mauritiana fiber and its epoxy composites, J. Ind. Text. (2020) 1–23, https://doi.org/10.1177/1528083720942614.

[14] G. Sv, R. I, S.S. N, Suitability assessment of raw-alkalized Ziziphus nummularia bark fibers and its polymeric composites for lightweight applications, Polym. Compos. 43 (2022) 5059–5075.

[15] V. Raghunathan, J.D.J. Dhilip, G. Subramanian, H. Narasimhan, C. Baskar, A. Murugesan, A. Khan, A. Al Otaibi, Influence of chemical treatment on the physico-mechanical characteristics of natural fibers extracted from the barks of Vachellia farnesiana, J. Nat. Fibers 19 (2022) 5065–5075, https://doi.org/10.1080/15440478.2021.1875353.

[16] Y.M. Tiwari, S.K. Sarangi, Characterization of raw and alkali treated cellulosic Grewia Flavescens natural fiber, Int. J. Biol. Macromol. 209 (2022) 1933–1942, https://doi.org/10.1016/j.ijbiomac.2022.04.169.

[17] S.V. Gurupranes, I. Rajendran, N. Shanmuga Sundaram, Suitability assessment of raw-alkalized Ziziphus nummularia bark fibers and its polymeric composites for lightweight applications, Polym. Compos. 43 (2022) 5059–5075, https://doi.org/10.1002/pc.26782.

[18] J.K. Singh, A.K. Rout, Characterization of raw and alkali - treated cellulosic fibers extracted from Borassus flabellifer L, Biomass Convers. Biorefinery (2022) 1–4, https://doi.org/10.1007/s13399-022-03238-x.

[19] A. Vinod, T.G. Yashas Gowda, R. Vijay, M.R. Sanjay, M.K. Gupta, M. Jamil, V. Kushvaha, S. Siengchin, Novel Muntingia Calabura bark fiber reinforced green-epoxy composite: a sustainable and green material for cleaner production, J. Clean. Prod. 294 (2021) 126337, https://doi.org/10.1016/j.jclepro.2021.126337.

[20] M. Jawaid, H.P.S.A. Khalil, A.A. Bakar, Woven hybrid composites : tensile and flexural properties of oil palm-woven jute fibres based epoxy composites, Mater. Sci. Eng. 528 (2011) 5190–5195, https://doi.org/10.1016/j.msea.2011.03.047.

[21] P. Madhu, M.R. Sanjay, M. Jawaid, S. Siengchin, A. Khan, C.I. Pruncu, A new study on effect of various chemical treatments on Agave Americana fiber for composite reinforcement: physico-chemical, thermal, mechanical and morphological properties, Polym. Test. 85 (2020) 106437, https://doi.org/10.1016/j.polymertesting.2020.106437.

[22] R. Vijay, D.L. Singaravelu, A. Vinod, M.R. Sanjay, S. Siengchin, Characterization of alkali-treated and untreated natural fibers from the stem of parthenium hysterophorus, J. Nat. Fibers 18 (2019) 80–90, https://doi.org/10.1080/15440478.2019.1612308.

[23] R. Srisuk, L. Techawinyutham, A. Vinod, S. Mavinkere Rangappa, S. Siengchin, Agro-waste from Bambusa flexuosa stem fibers: a sustainable and green material for lightweight polymer composites, J. Build. Eng. 73 (2023) 106674, https://doi.org/10.1016/j.jobe.2023.106674.

[24] V. A, S.M. Rangappa, R. Srisuk, J. Tengsuthiwat, A.R. R, S. Siengchin, Agro-waste Capsicum Annum stem: an alternative raw material for lightweight composites, Ind. Crops Prod. 193 (2023) 116141, https://doi.org/10.1016/j.indcrop.2022.116141.

[25] R. Vijay, D. Lenin Singaravelu, A. Vinod, M.R. Sanjay, S. Siengchin, M. Jawaid, A. Khan, J. Parameswaranpillai, Characterization of raw and alkali treated new natural cellulosic fibers from Tridax procumbens, Int. J. Biol. Macromol. 125 (2019) 99–108, https://doi.org/10.1016/j.ijbiomac.2018.12.056.

[26] A. Khan, R. Vijay, D.L. Singaravelu, M.R. Sanjay, S. Siengchin, F. Verpoort, K.A. Alamry, A.M. Asiri, Extraction and characterization of natural fiber from eleusine indica grass as reinforcement of sustainable fiber-reinforced polymer composites, J. Nat. Fibers (2019) 1–9, https://doi.org/10.1080/15440478.2019.1697993, 00.

[27] A. Vinod, R. Vijay, D.L. Singaravelu, M.R. Sanjay, S. Siengchin, Y. Yagnaraj, S. Khan, Extraction and characterization of natural fiber from stem of cardiospermum halicababum, J. Nat. Fibers (2019) 1–11, https://doi.org/10.1080/15440478.2019.1669514, 00.

[28] R. Vijay, S. Manoharan, S. Arjun, A. Vinod, D.L. Singaravelu, Characterization of silane-treated and untreated natural fibers from stem of leucas aspera, J. Nat. Fibers 18 (2020) 1–17, https://doi.org/10.1080/15440478.2019.1710651.

[29] S.K. Saw, K. Akhtar, N. Yadav, A.K. Singh, Hybrid composites made from jute/coir fibers: water absorption, thickness swelling, density, morphology, and mechanical properties, J. Nat. Fibers 11 (2014) 39–53, https://doi.org/10.1080/15440478.2013.825067.

[30] V.K. Kaushik, A. Kumar, S. Kalia, Effect of mercerization and benzoyl peroxide treatment on morphology, thermal stability and crystallinity of sisal fibers, Int. J. Textil. Sci. 1 (2013) 101–105, https://doi.org/10.5923/j.textile.20120106.07.

[31] V. Fiore, T. Scalici, A. Valenza, Characterization of a new natural fiber from Arundo donax L. as potential reinforcement of polymer composites, Carbohydr. Polym. 106 (2014) 77–83, https://doi.org/10.1016/j.carbpol.2014.02.016.

[32] S. Hossain, M.A. Jalil, T. Islam, M.M. Rahman, A low-density cellulose rich new natural fiber extracted from the bark of jack tree branches and its characterizations, Heliyon 8 (2022) 12345, https://doi.org/10.1016/j.heliyon.2022.e11667.

[33] R. Selvaraj, A. Maneengam, M. Sathiyamoorthy, Characterization of mechanical and dynamic properties of natural fiber reinforced laminated composite multiple-core sandwich plates, Compos. Struct. 284 (2022) 115141, https://doi.org/10.1016/j.compstruct.2021.115141.

[34] A.D. French, Increment in evolution of cellulose crystallinity analysis, Cellulose 27 (2020) 5445–5448, https://doi.org/10.1007/s10570-020-03172-z.

[35] S. Park, J.O. Baker, M.E. Himmel, P.A. Parilla, D.K. Johnson, Cellulose crystallinity index: measurement techniques and their impact on interpreting cellulase performance, Biotechnol. Biofuels 3 (2010) 1–10, https://doi.org/10.1080/02773818608085213.

[36] L. Segal, J.J. Creely, A.E. Martin, C.M. Conrad, An empirical method for estimating the degree of crystallinity of native cellulose using the X-ray diffractometer, Textil. Res. J. 29 (1959) 786–794, https://doi.org/10.1177/004051755902901003.

[37] H.N.C. Xue, K. Markus, B. Antje, P. Thomas, H. King, C.D. Delhom, S. Nam, J.V. Edwards, S.H. Kim, F. Xu, A.D. French, Effects of ball milling on the structure of cotton cellulose, Cellulose 26 (2019) 305–328, https://doi.org/10.1007/s10570-018-02230-x.

[38] L. Ding, X. Han, L. Cao, Y. Chen, Z. Ling, J. Han, S. He, S. Jiang, Characterization of natural fiber from manau rattan (Calamus manan) as a potential reinforcement for polymer-based composites, J. Bioresour. Bioprod. 7 (2022) 190–200, https://doi.org/10.1016/j.jobab.2021.11.002.

[39] O.Y. Keskin, S. Koktas, Y. Seki, R. Dalmis, G.B. Kilic, D. Albayrak, Natural cellulosic fiber from Carex panicea stem for polymer composites: extraction and characterization, Biomass Convers. Biorefinery (2022), https://doi.org/10.1007/s13399-022-03458-1.

[40] R.A. Alsulami, S.A. El-Sayed, M.A. Eltaher, A. Mohammad, K.H. Almitani, M.E. Mostafa, Thermal decomposition characterization and kinetic parameters estimation for date palm wastes and their blends using TGA, Fuel 334 (2023) 126600, https://doi.org/10.1016/j.fuel.2022.126600.

[41] M.O.S. Lobregas, E.V.D. Buniao, J.L. Leaño, Alkali-enzymatic treatment of Bambusa blumeana textile fibers for natural fiber-based textile material production, Ind. Crops Prod. 194 (2023), https://doi.org/10.1016/j.indcrop.2023.116268.

[42] R.F. Pereira Junio, L. De Mendonça Neuba, A.T. Souza, A.C. Pereira, L.F. Cassiano Nascimento, S.N. Monteiro, Thermochemical and structural characterization of promising carnauba novel leaf fiber (Copernicia prunifera), J. Mater. Res. Technol. 18 (2022) 4714–4723, https://doi.org/10.1016/j.jmrt.2022.04.127.

[43] I. Lalaymia, A. Belaadi, A. Bedjaoui, H. Alshahrani, M.K.A. Khan, Extraction and characterization of fiber from the flower stalk of the Agave plant for alternative reinforcing biocomposite materials, Biomass Convers. Biorefinery (2023), https://doi.org/10.1007/s13399-023-04782-w.
[44] N. Venkatachalam, P. Navaneethakrishnan, T.P. Sathishkumar, Characterization of novel Passiflora foetida natural fibers for paper board industry, J. Ind. Text. 2016 (2016) 1–24, https://doi.org/10.1177/1528083716682923.
[45] P. Senthamaraikannan, M. Kathiresan, Characterization of raw and alkali treated new natural cellulosic fiber from Coccinia grandis.L, Carbohydr. Polym. 186 (2018) 332–343, https://doi.org/10.1016/j.carbpol.2018.01.072.